

Domain patterns in incommensurate systems with the uniaxial real order parameter

V. Dananić

*Department of Physics, Faculty of Chemical Engineering and Technology, University of Zagreb,
Marulićev trg 19, 41000 Zagreb, Croatia*

A. Bjeliš

Department of Theoretical Physics, Faculty of Sciences, University of Zagreb, POB 162, 41001 Zagreb, Croatia
(Received 1 April 1994; revised manuscript received 8 June 1994)

The basic Landau model for the incommensurate-commensurate transition to the uniform or dimerized uniaxial ordering is critically reexamined. The previous analyses identified only sinusoidal and homogeneous solutions as thermodynamically stable and proposed a simple phase diagram with the first-order phase transition between these configurations. By performing the numerical analysis of the free-energy and the Euler-Lagrange equation we show that the phase diagram is more complex. It also contains a set of metastable solutions present in the range of coexistence of homogeneous and sinusoidal solutions. These new configurations are periodic patterns of homogeneous domains connected by sinusoidal segments. They are Lyapunov unstable, very probably due to the nonintegrability of the free-energy functional. We also discuss some other mathematical aspects of the model and compare it with the essentially simpler sine-Gordon model for the transitions to the states with higher commensurabilities. We argue that the present results might be a basis for the explanation of phenomena such as thermal hystereses, cascades of phase transitions, and memory effects.

PACS number(s): 64.70.Rh, 64.60.My

I. INTRODUCTION

During the past 15 years over a hundred materials [1–3] exhibiting incommensurate properties have been discovered. As the experience of a number of models show, the reason for the occurrence of incommensurate phases lies in the existence of two or more competitive interactions which prefer different periods of ordering. Depending on the relative strengths of interactions, the ordering may be incommensurate, commensurate, or chaotic. A simple example is the model of Frenkel and Kontorowa (FK) [4], studied so far by many authors [5]. It starts from a discrete harmonic array of atoms in a periodic background potential and may have any of the three types of ordering mentioned. In particular, if the background potential is large enough with respect to the harmonic one, the atoms arrange in a chaotic way. It is important, however, to stress that such chaotic features may be lost after the continuation of the original discrete space. For example, the continuation of the FK model leads in the lowest order to the sine-Gordon model, which is integrable and has no chaotic solutions.

On the other hand, the space continuation is a necessary step in the Landau expansion of the free energy. The latter is based on two approximations: the reduction of the summation in the reciprocal space to the narrow range around a given star of wave vectors and the truncation in the series of powers in the order parameter. While the choice of the star is related to the details of the competitive interactions, the introduction of the cutoffs in the wave vector summations is justified by the weakness

of these interactions. Indeed, only then can one exclude distances in the real space shorter than reciprocal cutoffs. The only short-range scales that remain are periods of fast modulations of order parameters, defined by the star of wave vectors itself.

The truncation of the power series in the Landau expansion is strictly justified only in the vicinity of the phase transition at the temperature T_I from the high temperature disordered state to the ordered one. Still, the Landau expansion sometimes gives a reasonably good description of the incommensurate-commensurate (IC) transitions also well below T_I . The range of its applicability depends on its microscopic origin. For example, for the anisotropic Ising model with nearest and next nearest neighbors (ANNNI) the Landau expansion, which follows after continuing both the space and the Ising variables, reproduces well only the transition line T_L [5,6]. On the other hand, the Landau expansions for electronically driven charge and spin density wave instabilities are useful as well in the range of lower temperatures below T_I . The well-known example is the rich phase diagram of the organic chain conductor tetrathiafulvalene-tetracyanoquinodimethane (TTF-TCNQ) [7].

In the Landau model the commensurate state below the critical temperature of the IC transition T_L is characterized by the star of wave vectors $\{\vec{q}_c\}$. The dimension of the order parameter is proportional to the number of arms in this star [8]. In most cases the order parameter is a multicomponent (e.g., complex) quantity. It may be a one component (i.e., real) quantity only when \vec{q}_c lies in the center or at the border of the Brillouin zone. The simplest, but still very frequent, cases which allow

both above possibilities are those with a uniaxial modulation characterized by a scalar physical quantity such as the local electron density in charge density waves, the atomic displacement along some fixed direction in ferroelectric systems, the magnetization along some preferred easy axis in magnetic systems, etc. The considerations in the present work will be limited to such uniaxial modulations.

As far as $q_0 \neq 0, \frac{1}{2}$, the star of wave vectors for a uniaxial ordering has two points ($\pm q_0$). The order parameter Ψ is then either complex (as is most often the case) or has an even number of components greater than two (e.g., six for the uniaxial spin density wave [9]). In the former case $\Psi = \rho e^{i\Phi}$, with ρ and Φ being the amplitude and phase which generally vary in space already in the stable equilibrium state. The Landau expansion with respect to the star ($\pm q_0$) contains, beside the isotropic invariants, a phase dependent umklapp term which appears when q_0 is close to the commensurate value $q_c = 2\pi/n$ ($n = 3, 4, \dots$). If one now concentrates on the portion of the phase diagram with the IC transition to $q = q_c$, it is most convenient to pass to the expansion with respect to the star ($\pm q_c$). After this transformation the umklapp term acquires the form $\rho^n [e^{in\Phi} + \text{c.c.}]$ [with $\Phi \equiv \phi + (q_0 - q_c)x$ being the phase with respect to q_c], and an additional Lifshitz invariant $\Psi \partial \Psi^* / \partial x - \Psi^* \partial \Psi / \partial x$ with the prefactor $\sim (q_0 - q_c)$ appears in the Landau expansion. The latter invariant is essential for the thermodynamics of the corresponding IC transition. If one neglects the space dependence of the amplitude ρ , the Euler-Lagrange (EL) equation for the stable configurations is a well-known sine-Gordon equation. The corresponding phase diagram shows a "weak" singularity at the continuous transition from the dilute lattice of solitons in Φ to the commensurate ($\Phi = cte$) configuration [10,11].

The approach via the above sine-Gordon model exhausts all IC transitions with $n > 2$ in the systems with weak interactions. Of course, the cases $n = 3$ and $n = 4$ are the most interesting, since the corresponding prefactors of $e^{in\Phi}$ terms contain powers of amplitude compatible with the isotropic ρ^4 term, which is unavoidable in any Landau expansion. For the same reason the terms coming from higher commensurabilities are less and less important as n increases. This is in contrast to the strong-coupling systems in which the discrete space dependence *a priori* includes all commensurabilities.

Two cases that are not covered by the sine-Gordon model are the homogeneous ordering with the periodicity of the underlying lattice [$n = 1$, i.e., $q_c = 0(\text{mod}2\pi)$] and the dimerization ($n = 2$, i.e., $q_c = \pi = -\pi(\text{mod}2\pi)$). In both cases the Landau expansion cannot have the Lifshitz invariant. Namely, the commensurate star now has only one point, so that the basic irreducible representation is one dimensional, defining a real order parameter. The notion of phase then loses its sense, since for a sinusoidal modulation the displacement is the same (for $n = 1$) or has the same absolute value (for $n = 2$) at all lattice sites. This value is the only quantity characterizing the ordered phase and as such represents the real order parameter u . Since, as indicated above, for $n = 1, 2$ all lattice sites are equivalent, a common generic Landau

expansion can be formulated for both cases. As will be seen in Sec. II, the essential feature of this expansion is the possible negative sign of the term proportional to the squared first derivative of the order parameter. In order to stabilize the expansion one then has to include the term with the squared second derivative. This completes a minimal model for the commensurate lock-ins with $n = 1, 2$. It can be extended by further possible invariants, depending on the details in particular physical systems. The present analysis, however, will be limited to the minimal model. Its main aim is to point out basic qualitative differences between IC transitions with $n = 1, 2$ and those with $n > 2$.

The division of uniaxial IC transitions into two classes, i.e., those with (class I) and without (class II) Lifshitz invariance, is well established in the literature [1,3,12,13]. While the sine-Gordon model, as a minimal one for the former class, can be completely integrated [10,11], the problem of integrability of the model for the latter class is far from being resolved. Mathematically, the models based on the Lagrangian with higher derivative terms are equivalent to the Hamilton problems with an unbounded kinetic part. Thus one misses a visualization of the corresponding solutions through some mechanical analogs. In spite of these difficulties, previous works (see, e.g., [12,14]) suggested a surprisingly simple phase diagram, even simpler than that of the sine-Gordon model. It includes only two homogeneous solutions $u = 0$ and $u = u_0$, representing the disordered and commensurately ordered configurations respectively and an (almost) sinusoidal solution $u(x)$ with an incommensurate wave number. The IC transition itself is of first order. As it was explicitly stated [12], this phase diagram does not contain configurations of the soliton-lattice type, in contrast to the corresponding phase diagram of the sine-Gordon model.

In the present work we start from the question of the possible presence of patterns consisting of alternating commensurate domains, i.e., of soliton lattices for the class II systems. Due to the aforementioned nontrivial mathematical properties of the EL equation, such periodic solutions might cover only tiny subsets in the complete space of solutions. Under these circumstances a rather careful numerical analysis is unavoidable. Combining two independent numerical methods, we find a new sequence of highly nonsinusoidal solutions having a form of domain patterns. They are locally stable (i.e., metastable) in the range of the control parameter in which the commensurate configuration is metastable ("superheated"). As will be argued below, the presence of these solutions substantially enriches the phase diagram and may have direct consequences on the IC transitions in real systems.

In Sec. II we formulate the Landau model for class II and discuss its mathematical properties. In Sec. III we introduce the systematization of periodic solutions and describe the numerical procedures for obtaining them. The structure of the phase diagram is presented in Sec. IV. Finally, in Sec. V we point out the differences between the IC transitions of class I and class II and discuss possible implications on the experimental properties of a few well-known materials from class II.

II. THE MODEL AND ITS MATHEMATICAL ASPECTS

The wave number for the uniaxial system with a real order parameter $u(x)$ is situated either at the center ($q_c = 0$ for $n = 1$) or at the border ($q_c = \pi$ for $n = 2$) of the first Brillouin zone. The simple transformation by which in the latter case the origin of the wave number is shifted by π/a enables the construction of the common Landau expansion for both cases. This transformation corresponds to the elimination of fast variations in the direct space, realized by passing from the “displacement” at the n th site d_n to $u_n = (-1)^n d_n$. Since u_n slowly varies on the lattice scale, just like the displacements in the $n = 1$ case, one may pass to the continuous space coordinate provided that the interactions are weak enough.

The essential property of the Landau expansion for the incommensurate order close to $n = 1$ or $n = 2$ follows from the dependence of the free-energy density on the wave number q . The quadratic part $f_2(q)$ has to be an even function of q . Thus, as long as local minima of $f_2(q)$ are at finite values $\pm q_0$, it has a shape of a bottle bottom, modeled by

$$f_2(q) = (a + cq^2 + \frac{1}{2}dq^4) u^2(q) \quad (2.1)$$

with $c < 0$ and $q_0^2 = -c/d$. Here $d > 0$ by assumption. The corresponding expression for the free-energy functional in the direct space is

$$f[u] = \frac{1}{2L} \int_{-L}^L \left[d \left(\frac{d^2 u}{dx^2} \right)^2 + c \left(\frac{du}{dx} \right)^2 + au^2 + \frac{1}{2}bu^4 \right] dx, \quad (2.2)$$

where L is some macroscopic length (“volume”). Here $b > 0$, so that the first and the fourth term in Eq. (2.2) ensure that the free-energy functional is bounded from below. The coefficients a and c depend on temperature and perhaps on some other physical parameter(s). It is expected that there is a physical regime in which both coefficients are negative. The model (2.2) may be also formulated in the frame of the Lifshitz point theory [15,14]. It is a minimal one since no higher-order derivative terms such as $(d^3 u/du^3)^2$, $u^2(du/dx)^2$, etc. are included.

It should be pointed out that the model (2.2) describes the crossover with the number of components of the order parameter passing from one (for $c > 0$) to two (for $c < 0$). The incommensurate ordering with the complex order parameter is achieved when the center (or the border) of the Brillouin zone is not inside the cutoffs of parabolas around the minima at $\pm q_0$ and so becomes irrelevant for the Landau expansion. This gradual change of type of the incommensurate ordering cannot be simulated by the model with the two-component order parameter, as it was proposed in Ref. [16]. These two models correspond to different physical situations, i.e., in the latter case the

commensurate state is already characterized by two types of displacements.

Direct considerations of the free-energy functional (2.2) do not give full insight into its stable configurations. Up to “surface” terms, it can be recast into the form

$$f[u] = \frac{1}{2L} \int_{-L}^L \left[d \left(\frac{d^2 u}{dx^2} - \frac{c}{2d} u \right)^2 + \left(a - \frac{c^2}{4d} \right) u^2 + \frac{1}{2}bu^4 \right] dx. \quad (2.3)$$

In reaching thermodynamic equilibrium, the first term in Eq. (2.3) “prefers” sinusoidal modulation of $u(x)$ with the wave vector $q = \sqrt{-c/2d}$, provided that $c < 0$. The remaining two terms would then stabilize the amplitude of the modulation, provided that $a - c^2/4d < 0$. This simple reasoning gives us an idea how and for what values of control parameters a and c incommensurate configurations could emerge. Indeed, the line $a = c^2/4d$ in the phase diagram for the free energy (2.2) represents the transition line between the disordered state $u(x) = 0$ and the incommensurate sinusoidal state with the wave vector $q = \sqrt{-c/2d}$. This conclusion is exact at the transition line. For $a < c^2/4d$ the modulation does not remain purely sinusoidal, so that the higher harmonic terms have to be included in order to reach a true minimum. Still, such terms represent only a small correction to both the free energy and the wave vector [14] (see also Sec. IV below). However, our numerical analysis will show that more complex periodic configurations, which minimize the free-energy functional well below the line $a = c^2/4d$, cannot be found as a mere extension of this almost sinusoidal configuration.

We proceed by considering some mathematical aspects of the problem. Since the coefficients b and d in Eq. (2.2) are positive by assumption, the order parameter and free-energy density are redefined by introducing

$$\begin{aligned} u(x) &= \sqrt{\frac{d}{b}} \bar{u}(x), \\ f &= \frac{d^2}{b} \bar{f}, \\ c &= d\bar{c}, \quad a = d\bar{a}, \end{aligned} \quad (2.4)$$

so that

$$\bar{f}[\bar{u}] = \frac{1}{L} \int_0^L \left[\left(\frac{d^2 \bar{u}}{dx^2} \right)^2 + \bar{c} \left(\frac{d\bar{u}}{dx} \right)^2 + \bar{a} \bar{u}^2 + \frac{1}{2} \bar{u}^4 \right] dx. \quad (2.5)$$

In what follows we shall omit the bar above the quantities appearing in Eq. (2.5).

The search for thermodynamically stable configurations $u(x)$ begins with the study of the EL equation for the functional (2.5) as the necessary condition which each such configuration has to obey. It reads

$$\frac{d^4 u}{dx^4} - c \frac{d^2 u}{dx^2} + a u + u^3 = 0. \quad (2.6)$$

The acceptable solutions $u(x)$ of this equation are those for which the corresponding eigenvalue equation

$$\frac{d^4 \eta(x)}{dx^4} - c \frac{d^2 \eta(x)}{dx^2} + [a + 3u^2(x)]\eta(x) = \lambda \eta(x) \quad (2.7)$$

with boundary conditions

$$\eta(0) = \eta(L) = 0, \quad \eta'(0) = \eta'(L) = 0 \quad (2.8)$$

generates only positive values of λ 's. This is the sufficient and necessary condition for the thermodynamic stability of the solution $u(x)$.

We are not aware of any method which would lead to a complete integration of Eq. (2.6). A straightforward analysis shows that it does not possess the Painlevé property, i.e., its movable singularities are not only simple poles in the complex x plane. The Laurent expansion of the solution which starts with a simple pole does not exist, so that logarithmic terms have to be included. In such cases one may try a general transformation of both the dependent (u) and independent (x) variables with the aim of finding the transformed differential equation which reveals the Painlevé property. We have not found any such transformation. Even if it exists, it would not prove the integrability of (2.6), but would give only a strong indication for it. So, from the point of view of the Painlevé analysis we cannot conclude anything about the integrability of Eq. (2.6), except that it leaves us with a strong impression of its probable nonintegrability. A similar impression emerges if one considers Eq. (2.6) as the Hamilton system of equations with two degrees of freedom. The integrability is then ensured by the existence of two invariants. One of them is the Hamiltonian given by

$$H = \frac{1}{2}u^4 + au^2 - cu'^2 - u''^2 + 2u'u'''. \quad (2.9)$$

However, we cannot either find or prove the existence of the second invariant.

Passing to the numerical analysis, we note at the beginning that Eq. (2.6) cannot be treated by a direct step-by-step integration. Namely, an *ad hoc* choice of initial conditions as a rule leads to the unbounded solution $u(x)$. The reason for such behavior can be traced to the fact that generally solutions which are thermodynamically stable are not orbitally stable [17]. The orbital stability is realized only as a neutral Lyapunov stability, i.e., with all four Lyapunov exponents being imaginary. Otherwise at least one of these exponents has a positive real part since $-\mu$ is, together with μ , also the eigenvalue of the corresponding linearized equation. Since the Runge-Kutta and similar methods of direct integration of Eq. (2.6) are inadequate for orbitally unstable solutions, we have to use another method, i.e., to minimize the free-energy functional on a given space of configurations and to check afterward to what extent the obtained solutions obey the EL equation [18]. This approach is tractable only for periodic configurations to which we limit further considerations.

III. PERIODIC SOLUTIONS

Any periodic configuration $u(x)$ with the period $2\pi/k$ can be expanded into a Fourier series

$$u(x) = a_0 + \sqrt{2} \sum_{n=1}^{\infty} [a_n \cos(nkx) + b_n \sin(nkx)] . \quad (3.1)$$

This series can be further simplified after noticing that the differential equation (2.6) is autonomous and invariant under reflections $x \rightarrow -x$ and $u \rightarrow -u$, so that the solutions may have additional symmetries. Let us distinguish between four classes: (i) configurations that are even with respect to both axes u and u' , (ii) configurations that are even with respect to the u axis only, (iii) configurations that are even with respect to the u' axis only, and (iv) configurations without any particular symmetry in the (u, u') plane.

For any periodic configuration $u(x)$ the functional (2.5) may be replaced by the functional

$$f[u(x)] = \frac{k}{2\pi} \int_0^{\frac{2\pi}{k}} [u''^2 + cu'^2 + au^2 + \frac{1}{2}u^4] dx, \quad (3.2)$$

with an error which vanishes as $1/L$ for large L . Replacing further the integration coordinate x by the coordinate

$$z = kx, \quad (3.3)$$

we come to the functional

$$f[u(z)] = \frac{1}{2\pi} \int_0^{2\pi} [k^4 u''^2 + ck^2 u'^2 + au^2 + \frac{1}{2}u^4] dz, \quad (3.4)$$

where $u' \equiv du/dz$, etc. Finally, inserting the Fourier expansion (3.1) into Eq. (3.2) we get

$$\begin{aligned} f[u(x)] &\equiv f(k, a_0, a_1, \dots) \\ &= \sum_{n=0}^{\infty} (k^4 n^4 + ck^2 n^2 + a) (a_n^2 + b_n^2) + \frac{1}{2} \langle u^4 \rangle, \end{aligned} \quad (3.5)$$

where

$$\langle (\dots) \rangle \equiv \frac{1}{2\pi} \int_0^{2\pi} (\dots) dz. \quad (3.6)$$

The functional (3.5) can be immediately minimized with respect to the wave vector k (note that $\langle u^2 \rangle$ and $\langle u^4 \rangle$ do not depend on k):

$$\frac{\partial f}{\partial k} = 0 \implies 2k \left[\sum_{n=1}^{\infty} (2k^2 n^4 + cn^2) (a_n^2 + b_n^2) \right] = 0, \quad (3.7)$$

i.e.,

$$k^2 \equiv k_0^2 = -\frac{c}{2} \frac{\sum_{n=1}^{\infty} n^2 (a_n^2 + b_n^2)}{\sum_{n=1}^{\infty} n^4 (a_n^2 + b_n^2)}. \quad (3.8)$$

We note that the wave vector k_0 from Eq. (3.8) is measured in units of $\sqrt{-c}$. Furthermore, the most interesting periodic solutions are expected when $c < 0$ and $a < -c^2/8$, since in this range the homogeneous configurations $u(x) = \pm\sqrt{-a}$ are stable. It is then natural to ask how homogeneous solutions participate in periodic solutions, i.e., whether the latter have ferromagnetic segments. In particular, we expect that ferromagnetic solutions and almost sinusoidal solutions could be mixed into new periodic configurations. Let us therefore limit further analysis to the range of parameters $c < 0, a < 0$ and introduce the following redefinitions:

$$k \equiv \sqrt{-c} q, \quad p \equiv -a/c^2, \quad (3.9)$$

$$a_n \equiv c\sqrt{p} A_n, \quad b_n \equiv c\sqrt{p} B_n, \quad n = 0, 1, 2, \dots$$

Note that $a < -c^2/8$ corresponds to $p > 1/8$. Then Eq. (3.5) reads

$$f(q, A_0, A_1, B_1, \dots)$$

$$= pc^4 \left[\sum_{n=0}^{\infty} (q^4 n^4 - q^2 n^2 - p) (A_n^2 + B_n^2) + \frac{p}{2} \langle v^4 \rangle \right]. \quad (3.10)$$

Here the function $v = v(z)$ is the Fourier expansion (3.1) with the amplitudes a_0, a_1, b_1, \dots replaced by the amplitudes A_0, A_1, B_1, \dots , etc. Note that p is the only control parameter which enters into the free energy.

The minimization [18] of the free-energy functional starts from a finite number of first harmonics with initial values chosen by some reasonable guess. During the variational steps, we enlarge the number of harmonics until the values of last harmonics are small enough (at least 10^{-13} times) in comparison with the first leading harmonics. In order to get periodic solutions, which will be shown in Sec. IV, we need at least 50 harmonics. Besides the periodic configuration $v(x)$ and the corresponding value of the free energy, we also obtain the wave number q_0 given by Eq. (3.8). Thus we have the complete characterization of a given periodic solution.

The configurations obtained satisfy well the EL equation (2.6). After inserting a given periodic solution, the left-hand side of Eq. (2.6) fluctuates irregularly as a function of z on a characteristic scale as small as 10^{-7} . The same conclusion follows from the second check in which we take a periodic solution as an initial approximation for the Newton-Kantorovich iteration. For this purpose we convert the Fourier expansion into a chosen basis of spline functions. The Newton-Kantorovich procedure ended, as a rule, after the first iteration [18].

The third numerical task concerns the local stability

of the obtained solutions. It is analyzed by diagonalizing the Hess determinant in the space of Fourier coefficients. Instead of being eliminated by making use of Eq. (3.8), the wave number is treated as an additional variable, since then the determinant can be much more easily calculated. As far as the lowest eigenvalue of this determinant is positive, the configuration is thermodynamically stable. The fact that the procedure does not involve multiperiodic solutions is based on the theory of normal forms [19]. Namely, in the range $p > 1/8$, which is of our primary concern, one pair of Lyapunov exponents for both homogeneous solutions $u = 0$ and $u = \pm\sqrt{-a}$ is not purely imaginary [17]. One concludes then that Eq. (2.6) has periodic solutions, but does not have multiperiodic solutions. The former thus cannot be unstable on account of the latter.

IV. PHASE DIAGRAM

It was already pointed out in the preceding section that $p = -a/c^2$ is the only combination of original physical parameters which remains after convenient redefinition of scales in the free-energy functional and the EL equation. Since the variations of parameters a and c are the most relevant for the IC transition, this means that all critical lines in the phase diagram represented by the (a, c) plane are parabolas determined by critical values of p . All parabolas meet with a common tangent at the origin $(0,0)$, named a ‘‘multicritical Lifshitz point’’ [14,20].

Further insight into the phase diagram can be gained from the dependence of the free energy on the parameter p for particular configurations. Let us rewrite the expression (3.10) in the form

$$f[v] = \frac{|a|c^2}{bd} \left\langle q^4 v'^2 - q^2 v^2 - p v^2 + \frac{|p|}{2} v^4 \right\rangle, \quad (4.1)$$

choose

$$f_0 = \frac{|a|c^2}{bd} \quad (4.2)$$

as the energy unit, and write $f/f_0 \rightarrow f$ further on. The free energy for the simplest homogeneous solutions

$$v = \pm 1 \quad (4.3)$$

then reads

$$f[\pm 1] = \frac{-p}{2}. \quad (4.4)$$

The approximate sinusoidal solution which figures in the phase diagrams of Refs. [14,20] is given by

$$v(z) \simeq \sqrt{2} \sqrt{\frac{2}{3p} \left(p + \frac{1}{4} \right)} \cos(z), \quad (4.5)$$

with the corresponding energy

$$\frac{f[v(z)]}{f_0} = -\frac{1}{3p} \left(p + \frac{1}{4} \right)^2 \quad (4.6)$$

and the “scaled” wave number

$$q^2 \simeq \frac{1}{2} \quad (4.7)$$

[the actual wave number is given by Eq. (3.9)]. The more precise result for this configuration, obtained through the minimization method of Sec. III, is presented in Table I(a) for $p = 1$. The solution $u(z)$ and its (u, u') section are shown in Fig. 1(a). As it was already stated in Ref. [14], the ratios $|a_3/a_1|$, $|a_5/a_1|$, etc. are rather small, while the values of a_1 and the free energy f are close to those given by Eqs. (4.5) and (4.6) (i.e., 0.9128 vs 0.913 and -0.523 , vs -0.5208 , respectively). Furthermore the numerical value of the parameter p for which the free energy becomes equal to the free energy of the homogeneous phase (4.3), i.e., for which the phase transition of the first order occurs, is

$$p_T \simeq 1.177, \quad (4.8)$$

again close to the approximate value 1.122. The wave vector corresponding to p_T is only slightly smaller than that given by Eq. (4.7). Furthermore the solution of Fig. 1(a) is thermodynamically stable for

$$p < p_C = 1.835, \quad (4.9)$$

which is close to the estimation $p_C = 2$ given in Ref. [14].

The homogeneous (4.3) and (almost) sinusoidal [Eq. (4.5) and Table I] configurations represent the skeleton of the phase diagram in the range $a < 0, c < 0$. Other, more complex, configurations bring a fine structure into this diagram. We start with a configuration belonging to class (ii), presented in Table I(b) and Fig. 1(b). The appearance of a small circle in Fig. 1(b) indicates that this configuration emerges through a local mix-

ing of the incommensurate sinusoidal configuration from Fig. 1(a) and the commensurate homogeneous configuration $v = 1$. Its free energy lies between the energies of these two configurations. The thermodynamic stability of this configuration is limited to a rather narrow range $p_L < p < p_R$ with $p_L = 0.956$ and $p_R = 1.05$. This is to be contrasted with the homogeneous configuration, which is stable for every $p \geq 1/8$, and the sinusoidal configuration, which is stable in the range $-1/4 \leq p \leq 1.835$. The wave number of the new configuration varies from $q(p_L) = 0.42$ to $q(p_R) = 0.4$, i.e., it is considerably smaller than the wave number of the sinusoidal configuration [Eq. (4.7)] everywhere in the domain of its stability. We also note that the right edge of stability is only slightly above the crossing of this line with that of the homogeneous ferromagnetic configuration (see also Fig. 3).

Next in the hierarchy of complexity is the configuration which again falls into class (i). It has two small circles in section plane (v, v') , one for each fixed point $v = \pm 1$. Since the mixing of the homogeneous and sinusoidal solution is even stronger in this case, the corresponding energy is higher than that of the configuration from Fig. 1(b). The representative of this configuration in the (x, v) and (v, v') planes is shown in Fig. 1(c). Again, the range of its stability is very narrow and approximately of the same width as that for the preceding configuration ($p_L = 0.8, p_R = 0.98$). The number of coefficients needed to accomplish the criterion established in Sec. III for this and further configurations is larger than 50. We do not present them for the sake of space.

The further two configurations falling into classes (i) and (ii) are shown in Figs. 1(d) and 1(e), respectively. The simplest configuration from class (iii) is shown in Fig. 1(f). Finally, in Fig. 1(g) we present one solution from class (iv). This solution has a lower symmetry than others. Namely, there is no point on the x axis with respect to which it is either even or odd, opposite to other solutions for which at least one such point exists. The configuration $u(x)$ belonging to class (iv) is different (in the sense given above) from $u(-x)$, but the free energies and the periods of both $u(x)$ and $u(-x)$ are the same.

All configurations presented [Figs. 1(a)–1(g)], and hopefully those more complex, could be viewed as being built from the following basic blocks: commensurate domains [left and right small circles in the section plane (v, v')] and the half-periods of the sinusoidal configuration [left and right halves of large ellipses in the section plane (v, v')]. Both types of blocks have, up to very slight deviations, the same lengths in all configurations derived. Thus we come to some kind of a nonlinear superposition principle. In that respect one can introduce a systematization of all periodic configurations by using the following scheme. Let us denote the blocks from Figs. 2(a), 2(b), 2(c), and 2(d) by letters s_+ , s_- , d_+ , and d_- , respectively. Any periodic configuration is then designated by a *word* in which the order of letters respects a simple rule by which a letter with a $+$ ($-$) subscript can be followed only by a letter with a $-$ ($+$) subscript. Taking this rule into account, one can further simplify the lettering by omitting subscripts. For example, the sinusoidal configuration from Fig. 1(a) is denoted by $\dots s_+ s_- s_+ s_- \dots$ or in a con-

TABLE I. The Fourier coefficients for the configurations s^2 (a) and sd (b).

n	A_n	n	A_n
(a)			
1	0.925	9	1.969×10^{-8}
3	-2.551×10^{-2}	11	-1.568×10^{-10}
5	2.444×10^{-4}	13	1.210×10^{-12}
7	-2.314×10^{-6}	15	-9.125×10^{-15}
(b)			
0	0.351	9	9.733×10^{-6}
1	0.794	10	4.385×10^{-6}
2	-0.381	11	-1.539×10^{-6}
3	7.873×10^{-3}	12	1.454×10^{-7}
4	3.323×10^{-2}	13	4.136×10^{-8}
5	-9.883×10^{-3}	14	-1.668×10^{-8}
6	6.204×10^{-4}	15	1.899×10^{-9}
7	3.960×10^{-4}	16	3.489×10^{-10}
8	-1.288×10^{-4}	17	-1.689×10^{-10}

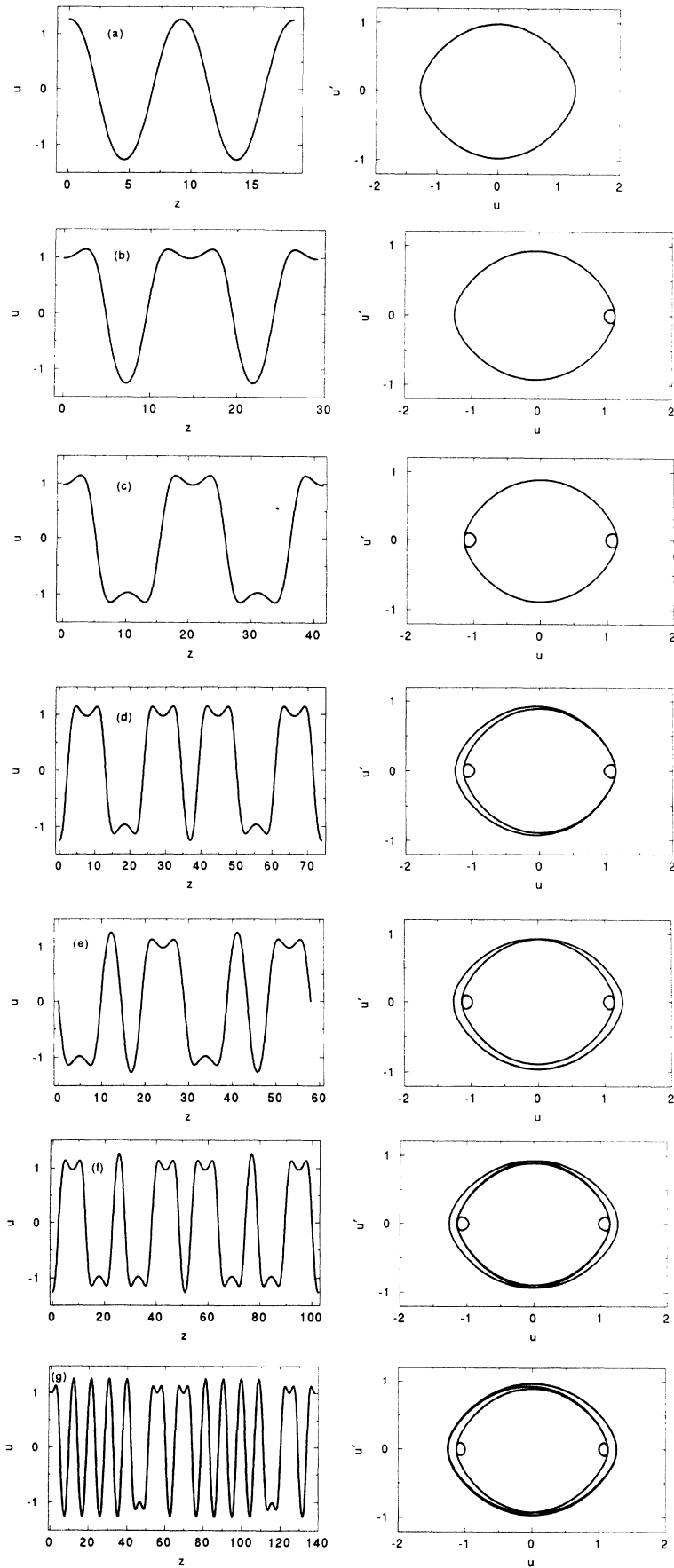


FIG. 1. $u(z)$ dependence (left) and (u, u') section (right) of the configurations s^2 (a), sd (b), d^2 (c), sd^3 (d), s^2d^2 (e), s^2d^4 (f), and s^9d^3 (g). For the configuration (c) $p = 0.9$ and for all other configurations $p = 1$. The symbolic words for configurations are defined in the text.

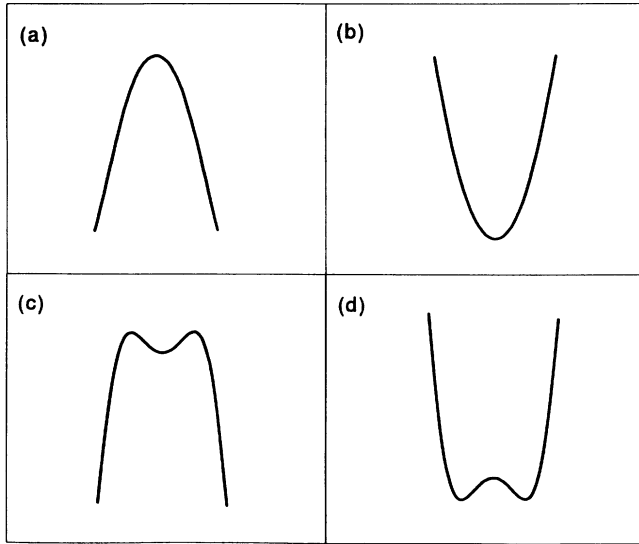


FIG. 2. The building blocks s_+ (a), s_- (b), d_+ (c), and d_- (d) for configurations from Fig. 1.

densed form $s_+s_- = s^2$, where the last word corresponds to one period of the configuration. Note that one condensed word must have an even number of letters. There are three different configurations with two-letter words, namely, $s_+s_- = s^2$, $s_+d_- = sd$, and $d_+d_- = d^2$. They are presented in Figs. 1(a), 1(b), and 1(c), respectively. The “four-letter” configurations are $s_+s_-s_+d_- = s^3d$, $s_+s_-d_+d_- = s^2d^2$, and $s_+d_-d_+d_- = sd^3$. We found two of these three configurations, i.e., the first [Fig. 1(d) and the second (Fig. 1(e)]. Finally, the word for the configuration from Fig. 1(g) has 12 letters and reads $s_-s_+s_-s_+s_-s_+s_-s_+d_-d_+s_-d_+ = s^9d^3$.

Unfortunately, at the present time we have no efficient numerical method which would enable the determination of a configuration which corresponds to any chosen word. Still, one could imagine a word with arbitrarily many letters, i.e., a sequence composed of sinusoidal and commensurate domains ordered in a random way inside one long period. In other words, the great freedom in the formation of macroscopic domain patterns may in principle still be interpreted in terms of the “determinism” presented in the EL equation (2.6). However, such patterns are obviously unreachable numerically. In this respect, we also mention that we did not find any configuration in which one commensurate domain is followed by another without inserting at least one half-sinusoidal block, i.e., a configuration which would have in the (u, u') section two small circles in succession. Furthermore, the commensurate domains with larger lengths could be expected for the parameters p larger than the value given by Eq. (4.8). However, it comes out that by adding more and more harmonics the wave number of such configurations does not stabilize to a finite value, but continuously goes to zero.

To summarize this section, we show in Fig. 3 the dependence of the free energy on the parameter p for all the solutions presented. The corresponding limits of stabil-

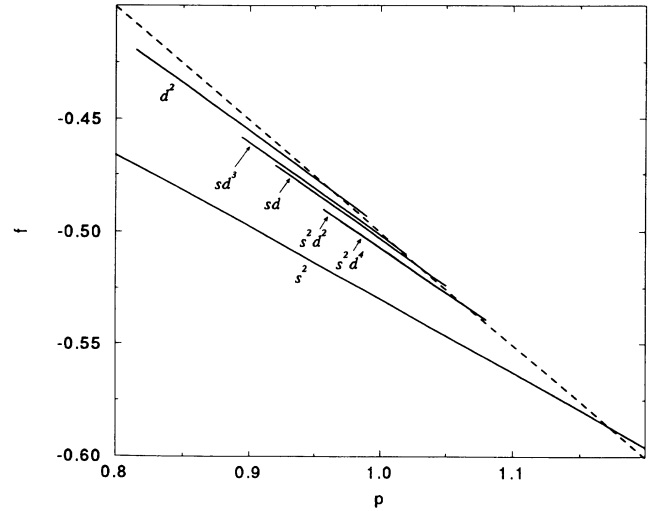


FIG. 3. The free energy f vs the control parameter p for the configurations from Figs. 1(a)–1(f) and for the homogeneous configuration (dashed line).

ity are gathered in Table II. Two lines, which dominate in Fig. 3, belong to the commensurate and sinusoidal configurations. The relevant range of values for p is limited from the left side by the edge of thermodynamic instability of commensurate configuration ($p > 1/8$) and from the right side by the critical value for the transition from the commensurate to the sinusoidal configuration ($p < 1.177$). Inside this range there are (probably infinitely) many relatively short lines belonging to periodic configurations composed of blocks from Fig. 2. As a rule, all these short lines cross the commensurate line on their right ends and cease to be thermodynamically stable immediately after crossing it.

In the recent analysis of the Landau model for the two-component ordering Aramburu *et al.* [16] showed that in the incommensurate configurations one of the components may have a soliton latticelike space dependence which resembles that shown in Fig. 1. Note, however, that these configurations belong to the single line in the phase diagram, which is equivalent to the line representing the sinusoidal configurations in Fig. 3.

The periods of the configurations from Table II are shown in Fig. 4. This diagram suggests that the separate curves are just parts of a smaller number (perhaps two) of curves representing multivalued dependences of

TABLE II. The values of parameter p for the left and right end points of stability ranges for the configurations from Figs. 1(a)–1(f).

Word	p_L	p_R
s^2	-0.25	1.835
sd	0.95661	1.082
d^2	0.815	0.989
sd^3	0.894	1.020
s^2d^2	0.970	1.080
s^2d^4	0.900	1.050

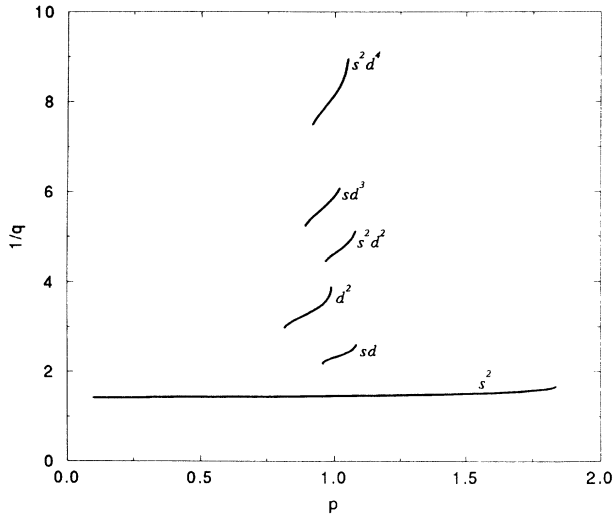


FIG. 4. The periods of configuration from Figs. 1(a)–1(d) vs the control parameter p .

the period on the parameter p . (Note that the periods of configurations with longer words would be situated higher in the diagram.) The missing parts on these curves would belong to unstable periodic configuration. Note that such configurations are out of scope of our numerical algorithm.

V. CONCLUSIONS

The discommensurations, i.e., the objects connecting commensurate domains with different or equal phases ($n \geq 3$) or signs ($n = 1, 2$), have a central role in the uniaxial IC transitions. The present analysis shows that in the systems of class II they enter into the phase diagram as ingredients of metastable configurations illustrated by Figs. 1(b)–1(g). As already pointed out in the preceding section, the discommensurations in these configurations just coincide with the local incommensurate order. Numerical results indicate that, as a rule, such configurations may be locally stable only within the range of coexistence of the homogeneous and the incommensurate (almost sinusoidal) ordered states. This is in contrast to class I, in which the sinusoidal incommensurate and the commensurate configurations do not coexist, but instead pass gradually from one to another through the continuous family of soliton lattices, with the phase solitons playing the role of discommensurations. By approaching the IC transition the distances between two phase solitons (i.e., the lengths of commensurate domains) tend towards infinity, so that a single discommensuration is well defined. It is also unique since there is only one type of separatrix which joins two hyperbolic fixed points which correspond to homogeneous (commensurate) state(s) in the sine-Gordon problem. Our numerical results suggest that this is not the case for class II, i.e., the isolated discommensurations do not appear as stable objects since all periodic domain configurations cease to be stable at

finite periodicities. In other words, although Eq. (2.6) has, e.g., solutions with a single solitary discommensuration, they are not thermodynamically stable. Furthermore, an isolated discommensuration is not uniquely defined since there are many ways to join two fixed points ($u = \pm 1, u' = u'' = u''' = 0$) in Figs. 1(b)–1(g) due to the complex Lyapunov exponents characterizing their stability.

The model (2.2) can be extended by further invariants [such as $u^2(du/dx)^2$], depending on their relevance in particular physical situations [3,13,21,22]. Such extensions increase the dimension of the parameter space and may lead to modifications in the phase diagram. Still, we do not expect that they alter our main conclusions presented in Fig. 3, which are closely related to the very probable nonintegrability of the functional (2.2). The integrability of the free-energy functional can be realized only for special (and thus marginal) values of parameters.

The presence of metastable configurations makes the IC transitions for class II more complex than it was thought before [3,13–15]. In fact, being the “droplet” states which mix two basic states of the first-order transition, these configurations complete in a natural way the phase diagram from Fig. 3. However, it should be stressed that they are purely intrinsic solutions of the EL equation for the free-energy functional (2.5). In other words, there is no need for some extrinsic inputs [such as boundaries, external field(s), defects, impurities, etc.], which are usually necessary for the stabilization of mixed states in the systems passing through the phase transition of the first order. However, this does not exclude possible additional extrinsic influences on the “microscopic” periodic configurations, which, as will be argued below, very probably take place in real systems.

Let us now consider possible physical implications of metastable lines in Fig. 3. At first, a direct identification of a periodic domain configuration in structural measurements implies a detailed knowledge of the corresponding structure factor. Our preliminary numerical computations suggest that the structure factors of domain configurations from Figs. 1(b)–1(g) and that of the sinusoidal configuration [Fig. 1(a)] are hardly distinguishable in the experimentally most interesting Brillouin zones with rather low Bragg indices. More noticeable differences are expected, however, in the zones with large indices in which the scattering from the domain configuration is on the fine scale more noisy than that from the sinusoidal configuration. Thus the structural identification of complex domain patterns could be a subtle experimental task. Still, if the commensurate and/or incommensurate segments are rather long, the corresponding structure factor has coexisting peaks at $q = 0$ and $q = \pm\sqrt{-c/2d}$. Such a coexistence of peaks was indeed observed in the neutron scattering measurements [23] on the diacetylene bis-*p*-toluene sulphonate of 2,4-hexadiyne-1,6 diol (PTS), the system which belongs to class II and passes through the Lifshitz point by gradual conversion from the monomer to the polymer crystal structure [24,25].

The physical properties of a given system are usually followed by varying one or two parameters, e.g., temper-

ature and another appropriate quantity such as pressure, strain, concentration of some constituent, degree of polymerization, etc. Any such variation can in principle be represented by a path in the $(a/b, c/d)$ plane, i.e., by some variation of the reduced control parameter p . Depending on the details of such a path (including its direction) and on other possible specific influences, the system may pass through a number of metastable periodic configurations, showing discontinuities in physical properties such as the staircase dependence on, e.g., temperature, the hysteresis behavior, the dependence on the initial state (i.e., history), etc. Such effects are indeed often met in the systems of class II [3], such as thiourea [26], ferroelectric materials such as barium sodium niobate (BSN) [28], and again PTS [23–25]. The hysteresis and memory effects in thiourea [27] and BSN [28] were most often interpreted by assuming that impurities are mobile enough to form a density wave as a response to the incommensurate lattice modulation, which in reverse tends to pin the modulation wave and to fix its position in the crystal [29,30]. On the contrary, the explanation of these effects based on the present analysis is essentially microscopic and universal for the whole class II of IC systems [31]. The defects (and/or other possible extrinsic causes) may still have a secondary role as triggers which favor the stabilization of some particular periodic domain patterns among all those available from the phase diagram from Fig. 3. Our explanation, however, does not invoke their mobility. Note that the dominant defects in some systems exhibiting a global hysteresis are by their nature immobile, such as, e.g., those in randomly polymerized crystals of PTS. The polymerization in PTS acts simultaneously as a control parameter (through the variation of the parameter c) and as a stabilization mechanism for domain patterns [25].

In conclusion we stress the theoretical significance of

the considered Landau model. When extended with transverse gradient terms, it represents the Landau expansion for, e.g., the ANNNI model in the vicinity of the Lifshitz point [6]. The phase diagram of Fig. 3 gives a new insight into this range of ANNNI phase diagram. Note that periodic domain patterns from Fig. 3 are not directly linked to the stable commensurate modulated configurations which appear far enough from the Lifshitz point in the ANNNI model [6]. Mathematical properties of the model considered here are particularly challenging. Besides being very probably nonintegrable, it has an unconventional classical mechanical counterpart with the kinetic energy which is not positively definite (in contrast to the class I models which do have such a counterpart because of the absence of higher derivative terms of the order parameters). As a consequence, the periodic solutions, which are especially important due to their thermodynamic stability, have a particular type of orbital instability. They seem to be immersed in a “chaotic web” which (again very probably due to the indefiniteness of the kinetic part of the Hamiltonian) is not even localized in the phase space. In that respect one encounters an intriguing open question of critical fluctuations in a purely (or quasi-) one-dimensional version of the model, for which the renormalization group expansion [15,22] cannot be applied. This and other previously mentioned extensions of the model are possible subjects of future investigations.

ACKNOWLEDGMENTS

We are indebted to E. Coffou and M. Rogina for help in the numerical analyses. A. B. acknowledges interesting conversations with D. K. Campbell and J. P. Pouget.

-
- [1] *Incommensurate Phases in Dielectrics*, edited by R. Blinc and A. P. Levanyuk (North-Holland, Amsterdam, 1986), Vols. 1 and 2.
 - [2] J. P. Pouget and R. Comès, in *Charge Density Waves in Solids*, edited by L. P. Gor'kov and G. Grüner (Elsevier Science, New York, 1989), p. 85.
 - [3] See, e.g., H. Z. Cummins, *Phys. Rep.* **185**, 211 (1990).
 - [4] Y. I. Frenkel and T. Kontorowa, *Zh. Eksp. Teor. Fiz.* **8**, 1340 (1938).
 - [5] See, e.g., Per Bak, *Rep. Prog. Phys.* **45**, 587 (1982).
 - [6] W. Selke, *Phys. Rep.* **170**, 214 (1988).
 - [7] S. Barišić and A. Bjeliš, in *Theoretical Aspects of Band Structure and Electronic Properties of Pseudo-One-Dimensional Solids*, edited by H. Kamimura (Riedel, Dordrecht, 1985), p. 49.
 - [8] L. D. Landau and E. M. Lifshitz, *Statistical Physics*, 2nd ed. (Pergamon, London, 1968).
 - [9] A. Bjeliš and D. Zanchi, *Phys. Rev. B* **49**, 5968 (1994).
 - [10] W. L. McMillan, *Phys. Rev. B* **14**, 1496 (1976).
 - [11] L. N. Bulaevskii and D. I. Khomskii, *Zh. Eksp. Teor. Fiz.* **74**, 1863 (1978) [*Sov. Phys. JETP* **76**, 971 (1978)].
 - [12] A. D. Bruce and R. A. Cowley, *J. Phys. C* **11**, 3609 (1978); A. D. Bruce, R. A. Cowley, and A. F. Murray, *ibid.*, p. 3591 (1978).
 - [13] J. C. Toledano and P. Toledano, *The Landau Theory of Phase Transitions* (World Scientific, Singapore, 1987).
 - [14] A. Michelson, *Phys. Rev. B* **16**, 577 (1977).
 - [15] R. M. Hornreich, M. Luban, and S. Shtrikman, *Phys. Rev. Lett.* **35**, 1678 (1975).
 - [16] L. Aramburu, G. Madariaga, and J. M. Perez-Mato, *Phys. Rev. B* **49**, 802 (1994).
 - [17] In the case of homogeneous solutions the thermodynamic stability goes together with the orbital instability. Taken $c < 0$, $u(x) = 0$ is thermodynamically stable for $a > c^2/4$ and orbitally stable for $a < c^2/4$. (For $a < 0$ this solution becomes orbitally unstable.) The corresponding ranges for $u(x) = \pm\sqrt{-a}$ are $a < -c^2/8$ and $a > -c^2/8$.
 - [18] V. Dananić, A. Bjeliš, M. Rogina, and E. Coffou, *Phys. Rev. A* **46**, 3551 (1992).
 - [19] Yu. N. Bibikov, in *Local Theory of Nonlinear Analytic Ordinary Differential Equations*, edited by A. Dold and B. Eckmann, *Lecture Notes in Mathematics* Vol. 702 (Springer, Berlin, 1979).
 - [20] A. Aharony, E. Domany, and R. M. Hornreich, *Phys. Rev. B* **36**, 2006 (1987).
 - [21] Y. Ishibashi and H. Shiba, *J. Phys. Soc. Jpn.* **45**, 409

- (1978).
- [22] H. J. Fishbeck, *Phys. Status Solidi B* **118**, 595 (1983).
- [23] J. P. Aimé, J. Lefebvre, M. Bentault, M. Schott, and J. T. Williams, *J. Phys. (Paris)* **43**, 307 (1982).
- [24] J. N. Patillon, P. Robin, P. A. Alboy, J. P. Pouget, and R. Comès, *Mol. Cryst. Liq. Cryst.* **76**, 297 (1987).
- [25] J. P. Pouget, *Europhys. Lett.* **11**, 645 (1990).
- [26] F. Denoyer and R. Currat, in *Incommensurate Phases in Dielectrics* (Ref. [1]), p. 129.
- [27] J. P. Jamet and P. Lederer, *J. Phys. (Paris) Lett.* **44**, L257 (1983).
- [28] J. C. Toledano, J. Schneck, and G. Errandonea, in *Incommensurate Phases in Dielectrics* (Ref. [1]), p. 233.
- [29] P. Lederer, J. P. Jamet, and G. Montambaux, *Ferroelectrics* **66**, 25 (1986).
- [30] G. Errandonea, *Phys. Rev. B* **33**, 6261 (1986).
- [31] The global hysteresis in systems which do not belong to the II class can be also interpreted as a microscopic phenomenon already in the weak coupling limit, after including in the sine-Gordon model at least two dominating commensurate potentials with different periods. A. Bjeliš and M. Latković (unpublished).